Model for the rotational contribution to quasielastic neutron scattering spectra from supercooled water

Li Liu,[1] Antonio Faraone,[1,2] and Sow-Hsin Chen[1,*]
[1]*Department of Nuclear Engineering, Massachusetts Institute of Technology, Cambridge, Massachusetts 02139*
[2]*Department of Physics and INFM, University of Messina, 98166 Messina, Italy*
(Received 21 December 2001; published 8 April 2002)

A model is proposed for the first-, second-, and third-order rotational correlation functions that are required for the computation of the rotational intermediate scattering function for the calculation of incoherent quasielastic neutron scattering (QENS) spectra from supercooled water. The model is tested against molecular-dynamics data generated from an extended-simple-point-charge model of water and is found to be satisfactory. The model can be used as a practical method for extracting rotational relaxation parameters from QENS spectra measured at large Q from supercooled bulk water or interfacial water in porous materials.

DOI: 10.1103/PhysRevE.65.041506 PACS number(s): 61.20.Lc, 61.12.Ex, 61.20.Ja

I. INTRODUCTION

Incoherent quasielastic neutron scattering (QENS) is a well established and a powerful method for studying translational and rotational dynamics of water molecules in bulk or in confinement [1–4]. Owing to the very large incoherent scattering cross section of a hydrogen atom as compared to that of an oxygen atom, the scattered signal from water is dominated by the incoherent scattering processes from the two hydrogen atoms in the molecules. As a result, a quasielastic scattering experiment from water is particularly suited for studying the single-particle dynamics of water molecules, which includes both molecular scale translational diffusion and rotational relaxation of the molecules in condensed states.

A QENS spectrum is proportional to the self-dynamic structure factor of the hydrogen atom $S_H(Q,\omega)$, which is the time Fourier transform of the intermediate scattering function (ISF) $F_H(Q,t)$. Here, Q denotes the magnitude of the scattering vector, and $E=\hbar\omega$, the energy transfer in the scattering process. Hence it is a usual practice in the literature to discuss the theoretical model for interpreting a QENS experiment in terms of the ISF [1]. We have previously discussed the validity of the so-called decoupling approximation for the intermediate scattering function of the hydrogen atom in water [5–7]

$$F_H(Q,t)=F_T(Q,t)F_R(Q,t), \tag{1}$$

where $F_T(Q,t)$, alternatively also called $F_{c.m.}(Q,t)$, and $F_R(Q,t)$ are, respectively, the translational ISF of the center of mass and that of the rotation around the center of mass of the molecule. In the extended-simple-point charge SPC/E model of water, the decoupling approximation is shown to be good at smaller Q (for $Q<1$ Å^{-1}). But the deviation increases to about 9% at an intermediate time for larger Q($Q\sim 2$ Å^{-1}) [6]. For QENS data analysis, in practice, this level of accuracy is acceptable, considering the typical error bars inherent in the data and in view of the fact that any other choices of the approximation will lead to an intractable complication. In this paper, we therefore use the decoupling approximation as a starting point of our analysis.

In a typical QENS experiment, one uses, say, 6 Å incident neutrons in a multidetector time-of-flight spectrometer, covering a Q range of 0.25 Å$^{-1}<Q<2.0$ Å^{-1}. In the range $Q<1$ Å^{-1}, one essentially measures just the translational part, $F_T(Q,t)$ alone, because it can be shown that the rotational ISF is nearly unity in this Q range [1]. For the range $Q>1$ Å^{-1}, the rotational ISF $F_R(Q,t)$ begins to become appreciably different from unity. Thus, in order to detect the rotational relaxation parameters, one has to take data at large Q range. In the following section, we shall describe a method of computing the rotational contribution to the spectra measured in a QENS experiment. In the literature on single-particle dynamics of water, it has been a usual practice to calculate $F_T(Q,t)$ by a jump diffusion and $F_R(Q,t)$ by rotational diffusion models, following the work by Teixeira, Bellissent-Funel, Chen, and Dianoux in 1985 [7]. However, it was shown in a recent paper by Chen *et al.* [6] that these two simple models were poor approximations for low-temperature water. In order to extract realistic relaxational parameters for both the translational and rotational motions in supercooled water from a QENS experiment, more accurate models for both the ISF's are necessary. We have proposed some time ago a ''relaxing cage model'' for the translational ISF [8] $F_T(Q,t)$, which was shown to be accurate for low-Q QENS data [9]. The present paper presents a model for the rotational ISF $F_R(Q,t)$.

II. THE MODEL

In a QENS experiment of water, the measured double-differential cross section is given by

$$\frac{d^2\sigma_{inc}}{d\Omega d\omega}=N\frac{2\sigma_H}{4\pi}\frac{k_f}{k_i}S_H(Q,\omega), \tag{2}$$

where N is the number of water molecules in the sample σ_H is the incoherent scattering cross section of a hydrogen atom, and k_f and k_i are, respectively, the wave numbers of the

*Author to whom correspondence should be addressed. Electronic address: sowhsin@mit.edu

 ©2002 The American Physical Society

scattered and incident neutrons. The self-dynamic structure factor $S_H(Q,\omega)$ of the hydrogen atom is given in terms of the ISF of the hydrogen by a Fourier transform

$$S_H(Q,\omega)=\frac{1}{2\pi}\int_{-\infty}^{\infty}dte^{i\omega t}F_H(Q,t). \tag{3}$$

$F_H(Q,t)$ is then the primary quantity of theoretical interest related to the experiment and can be calculated in a straightforward way by an molecular-dynamics (MD) simulation of a model water as well. $F_H(Q,t)$, in this paper, is given by the product of $F_T(Q,t)$ and $F_R(Q,t)$. We shall describe first an accurate method for the calculation of $F_T(Q,t)$, called relaxing cage model [8].

In the relaxing cage model, the translational ISF is given by

$$F_T(Q,t)=F_V(Q,t)\exp\left[-\left(\frac{t}{\tau_t}\right)^{\beta}\right], \tag{4}$$

where the vibrational part of the ISF is given by

$$F_V(Q,t)=\exp\left\{-Q^2v_0^2\left[\frac{1-C}{\omega_1^2}(1-e^{-\omega_1^2t^2/2})+\frac{C}{\omega_2^2}(1-e^{-\omega_2^2t^2/2})\right]\right\}. \tag{5}$$

In this expression, $\sqrt{2}\omega_1$ and $\sqrt{2}\omega_2$ are frequencies of the two characteristic peaks in the translational density of states of the center of mass, and C is the relative strength of the two peaks. It should be noted that at long-time limit (longer than 1 ps), this vibrational ISF decays to a plateau given by a Debye-Waller factor $A(Q)$

$$A(Q)=\exp\left\{-Q^2v_0^2\left[\frac{1-C}{\omega_1^2}+\frac{C}{\omega_2^2}\right]\right\}=\exp(-\tfrac{1}{3}Q^2a^2). \tag{6}$$

Both MD and QENS experiments gave the value of the mean-square vibrational amplitude, $a=0.5$ Å, in the supercooled region [10,11]. It is clear from the inspection of Eq. (4) that $F_V(Q,t)$ factor represents contribution to the ISF, coming from the in-cage (hydrogen-bonded first neighbor shell) vibrational motions of the center of mass of the central molecule, and the second stretch exponential factor represents the relaxation of the surrounding cage at long time.

A. Theory for the rotational *ISF*, $F_R(Q,t)$

We start from an exact expansion of the rotational ISF due to Sears [12]. Let $\vec{b}(t)$ denotes a vector from the center of mass to the hydrogen atom. This vector will acquire a time dependence as the water molecule rotates around the center of mass

$$F_R(Q,t)\equiv\langle e^{-i\vec{Q}\cdot\vec{b}(0)}e^{i\vec{Q}\cdot\vec{b}(t)}\rangle=j_0^2(Qb)+\sum_{\ell=1}^{\infty}(2\ell+1)j_\ell^2(Qb)C_\ell(t), \tag{7}$$

where $j_\ell(x)$ is the ℓth-order spherical Bessel function, $C_\ell(t)$ is the ℓth order rotational correlation function, and $b=0.98$ Å, which is approximately the length of the O-H bond in a water molecule. This expansion is very useful for a typical Q range encountered in QENS experiments, for which generally $Q<2.5$ Å^{-1}. In this case, the expansion needs to be carried out to at most $\ell=3$ terms. The advantage of using this expansion is that the Q dependence of the rotational ISF is exactly given and one needs to make a model for a few lower-order rotational correlation functions, which are Q-independent quantities. In this paper, we shall make a model explicitly for the function $C_1(t)$ and shall generate the other higher-order rotational correlation functions approximately using the maximum entropy method of Berne *et al.* [13].

The ℓth order rotational correlation function is defined as

$$C_\ell(t)=\langle P_\ell(\cos\theta(t))\rangle, \tag{8}$$

where $\theta(t)$ is the angle between the vector $\vec{b}(0)$ and $\vec{b}(t)$. We shall use a notation, $\mu(t)=\cos\theta(t)$. To calculate the statistical average, denoted by the pointed brackets, in Eq. (8), we need a probability distribution function $P(\mu,t)$. We shall consider the short-time behavior of $C_1(t)$ first. Imagine that at a given instance, say $t=0$, a typical hydrogen atom is hydrogen bonded to its nearest-neighbor oxygen atom. The short-time dynamics of the rotation of the vector $\vec{b}(t)$ around the center of mass must be well described by a harmonic motion of the angle $\theta(t)$, that is to say

$$\ddot{\theta}(t)+\omega^2\theta(t)=0. \tag{9}$$

Then it follows that the distribution function of $\theta(t)$ is Gaussian and the following Bloch theorem [14] holds:

$$\langle e^{\alpha\theta}\rangle=\exp[\tfrac{1}{2}\langle(\alpha\theta)^2\rangle]. \tag{10}$$

Using this theorem, one can then derive the following results:

$$C_1^s(t)=\langle\cos\theta(t)\rangle=\left\langle\frac{e^{i\theta}+e^{-i\theta}}{2}\right\rangle=\exp[-\tfrac{1}{2}\langle\theta^2(t)\rangle]. \tag{11}$$

Now since the tip of the vector $\vec{b}(t)$ is tracing a surface of a sphere of radius b centered around the center of mass, the arc that it traces at short time $\Delta\vec{b}(t)$ can be considered as a vector in a tangential plane, therefore, one can approximately write, $\theta^2=(1/b^2)(\Delta b_x^2+\Delta b_y^2)=[\int_0^t dt'\,\omega_x(t')]^2+[\int_0^t dt'\,\omega_y(t')]^2$, where $\vec{\omega}(t)=(1/b)[d\vec{b}(t)/dt]=d\vec{\theta}/dt$ is the angular velocity of the hydrogen atom around the center of mass. Next, using the identity

TABLE I. Simulated state points.

T (k)	ρ_s (g/cm^3)	E (kJ/mol)	P (MPa)	$D(10^{-5}$ cm^2/s)
284.5	0.984	-48.1	-73 ± 11	$(1.3\pm0.1)\times10^{0}$
250.0	0.986	-50.0	-76 ± 12	$(5.2\pm0.5)\times10^{-1}$
225.0	0.984	-52.6	-75 ± 15	$(4.4\pm0.4)\times10^{-2}$

$$\left\langle \left[\int_0^t dt' \omega_x(t') \right]^2 \right\rangle = \left\langle \int_0^t dt' \int_0^t dt'' \omega_x(t') \omega_x(t'') \right\rangle = 2 \int_0^t (t-\tau) \langle \omega_x(0) \omega_x(\tau) \rangle d\tau \quad (12)$$

we finally arrive at a result [15]

$$C_1^s(t) = \exp\left[- \int_0^t (t-\tau) \langle \omega_x(0) \omega_x(\tau) + \omega_y(0) \omega_y(\tau) \rangle d\tau \right] = \exp\left[- \frac{2}{3} \int_0^t (t-\tau) \langle \vec{\omega}(0) \cdot \vec{\omega}(\tau) \rangle d\tau \right]. \quad (13)$$

Define the normalized angular velocity autocorrelation function, $\psi_R(t) = \langle \vec{\omega}(0) \cdot \vec{\omega}(t) \rangle / \langle \omega^2 \rangle$, and its spectral density function by

$$Z_R(\omega) = \frac{1}{\pi} \int_{-\infty}^{\infty} e^{i\omega t} \psi_R(t) dt, \quad (14)$$

which is normalized to 1 for ω from 0 to ∞. Then the short-time approximation of the first-order rotational correlation function can be written as

$$C_1^s(t) = \exp\left[- \frac{4}{3} \langle \omega^2 \rangle \int_0^{\infty} d\omega Z_R(\omega) \frac{1-\cos(\omega t)}{\omega^2} \right]. \quad (15)$$

From the inspection of the MD-generated $Z_R(\omega)$ (see Fig. 2), we shall model the spectral density function by a simple Gaussian-like function

$$Z_R(\omega) = \frac{2\omega^6}{15\omega_3^6 \sqrt{2\pi\omega_3^2}} \exp\left[- \frac{\omega^2}{2\omega_3^2} \right], \quad (16)$$

where the peak position is located at $\sqrt{6}\omega_3$. The MD data show that this so-called hindered rotation peak is located approximately at 70 meV, fairly independent of temperature. In this model the short-time part of the first-order rotational correlation function can be written as

$$C_1^s(t) = \exp\left\{ - \frac{2}{3} \langle \omega^2 \rangle \int_0^{\infty} d\omega Z_R(\omega) \frac{1-\cos(\omega t)}{\omega^2} \right\} = \exp\left\{ - \frac{4\langle \omega^2 \rangle}{45\omega_3^2} [3(1-e^{-\omega_3^2 t^2/2}) + 6\omega_3^2 t^2 e^{-\omega_3^2 t^2/2} - \omega_3^4 t^4 e^{-\omega_3^2 t^2/2}] \right\}. \quad (17)$$

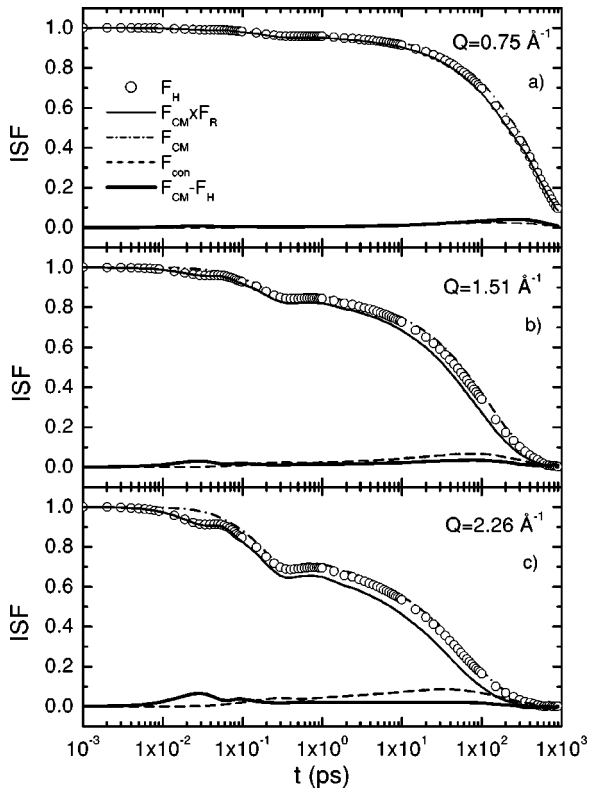

FIG. 1. The intermediate scattering functions (ISF) at three Q values (7.54 nm^{-1}, 15.1 nm^{-1}, and 22.6 nm^{-1}) and at $T=225$ K, as a function of the time in logarithmic scale. The open circles represent $F_H(Q,t)$; the dash-dot line, $F_{c.m.}(Q,t)$; the solid line, $F_{c.m.}(Q,t)F_R(Q,t)$; the dash line, the connected part of the correlation function, $F_{con}(Q,t)$ and the thick solid line, the difference, $F_{c.m.}(Q,t)-F_H(Q,t)$. It is to be noted that at low Q, the decoupling approximation is good but at high Q, the approximation progressively becomes poorer at long times but the deviation never exceeds 0.09. However, it is also noticeable that at long times ($t>1$ ps) F_H nearly coincides with $F_{c.m.}$.

This function $C_1^s(t)$ describes the short-time behavior of the first-order rotational correlation function. It starts from unity at $t=0$, exhibits an oscillation at time 0.05 ps and then decays to a flat plateau determined by $\exp(-4\langle \omega^2 \rangle / 15\omega_3^2)$ for times longer than 0.1 ps.

The relaxation at longer times can be described by an α relaxation model, which describes the relaxation of the cage surrounding the central water molecule. Thus the expression for $C_1(t)$ in the entire time range is given as

$$C_1(t) = C_1^s(t) \exp[-(t/\tau_R)^{\beta_R}]. \quad (18)$$

The whole picture resembles the relaxing cage model of the translational dynamics. At short times, the orientation of the central water molecule is fixed by the H bonds with its neighbors. It performs nearly harmonic oscillations around the hydrogen-bond direction. This dynamics is described by $C_1^s(t)$. At longer times, the bonds break and the cage begins to relax. So the particle can reorient itself, losing memory of

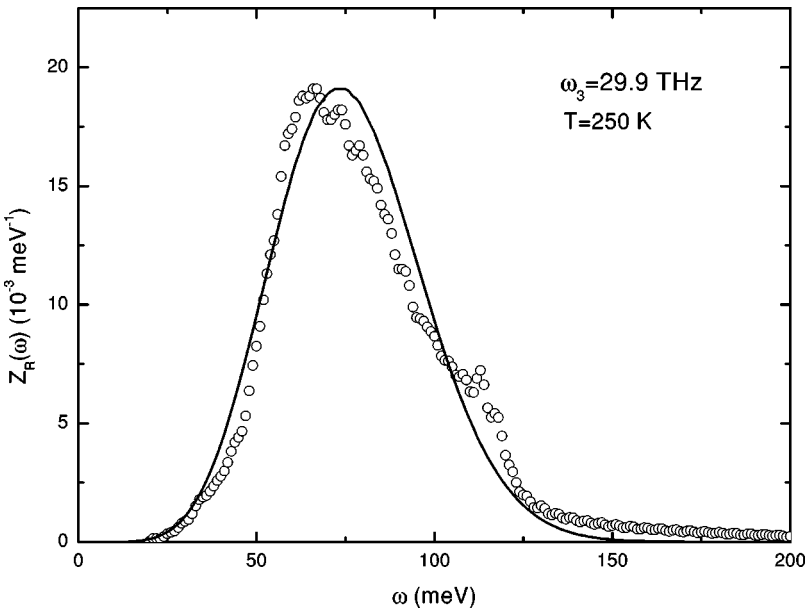

FIG. 2. Spectral density function of the normalized angular velocity autocorrelation function $Z_R(\omega)$ at $T=250$ K. The open circles represent the results of the simulation and the solid line, the resulting fit by the model Eq. (16).

its initial orientation. Thus the first-order rotational correlation function eventually decays to zero by a stretched exponential relaxation.

To calculate $C_2(t)$ and $C_3(t)$ from $C_1(t)$, we need to know the functional form of the distribution function $P(\mu,t)$. We shall guess the distribution function based on maximization of the informational entropy subjected to a condition that we know $C_1(t)$ [13]. According to the scheme, the distribution function is given by

$$P(\mu,t)=e^{\alpha+\beta\mu}. \tag{19}$$

Because $\int d\Omega P(\mu,t)=1$,

$$e^{\alpha}=\frac{1}{2\pi}\frac{\beta}{e^{\beta}-e^{-\beta}}, \tag{20}$$

$$C_1(t)=\int d\Omega e^{\alpha+\beta\mu}\mu=-[1/\beta(t)]+\coth\beta(t). \tag{21}$$

The higher-order correlation functions are determined from $C_1(t)$ using Eqs. (19)–(21). The connection of $C_1(t)$ to the higher order rotational correlation functions is given in terms of $\beta(t)$. The results are

$$C_2(t)=1-[3/\beta(t)]C_1(t), \tag{22}$$

$$C_3(t)=-\frac{5}{\beta(t)}+\left[1+\frac{15}{\beta^2(t)}\right]C_1(t). \tag{23}$$

B. SPC/E simulation

We use MD simulation data of water to test out our model for the rotational correlation functions. This is a more suitable method for testing the analytical theory than using real neutron scattering data, since MD data do not have the complication of the resolution effect present in real experimental data. We carried out an extensive simulation, in an NVE ensemble with 216 water molecules contained in a cubic box of an edge 18.65 Å. The effective potential used is the SPC/E. This potential treats a single water molecule as a rigid set of point masses with an OH distance of 0.1 nm and an HOH angle equal to the tetrahedral angle 109.47°. The point charges are placed on the atoms and their magnitudes are $q_H=0.4238e$ and $q_O=-2q_H=-0.8476e$. Only the oxygen atoms in different molecules interact among themselves via a Lennard-Jones potential, with the parameters $\sigma=0.31656$ nm and $\epsilon=0.64857$ kJ/Mol. The interaction between pairs of molecules is calculated explicitly when their separation is less than a cutoff distance r_c of 2.5σ. The contribution due to Coulomb interactions beyond r_c is calculated using the reaction-field method, as described by Steinhauser [16]. Also, the contribution of Lennard-Jones interactions between pairs separated by more than r_c is included in the evaluation of thermodynamic properties by assuming a uniform density beyond r_c. A heat bath [17] has been used to allow for heat exchange while changing temperature of the system. After the system has been equilibrated, the heat bath is then removed. In our simulation, periodic boundary conditions are used. The time step for the integration of the molecular trajectories is 1 fs. Simulations at low T were started from equilibrated configurations at higher T. Equilibration was monitored via the time dependence of the potential energy. In all cases the equilibration time t_{eq} was longer than the time needed to enter the diffusive regime. We studied three temperatures, 284.5 K, 250.0 K, and 225.0 K. We note that for the ESPC model of water, the density maximum occurs at about 250 K, which corresponds to 277 K in the real water. For the lowest temperature, 225 K, we recorded water trajectories for more than 1 ns. And for the other two temperatures we recorded for 0.1 ns. Further detailed thermodynamic parameters of the simulations are given in [11,10].

The SPC/E potential has been explicitly parametrized to reproduce the experimental value of the self-diffusion constant at ambient temperature and at a density of 1 g/cm^3

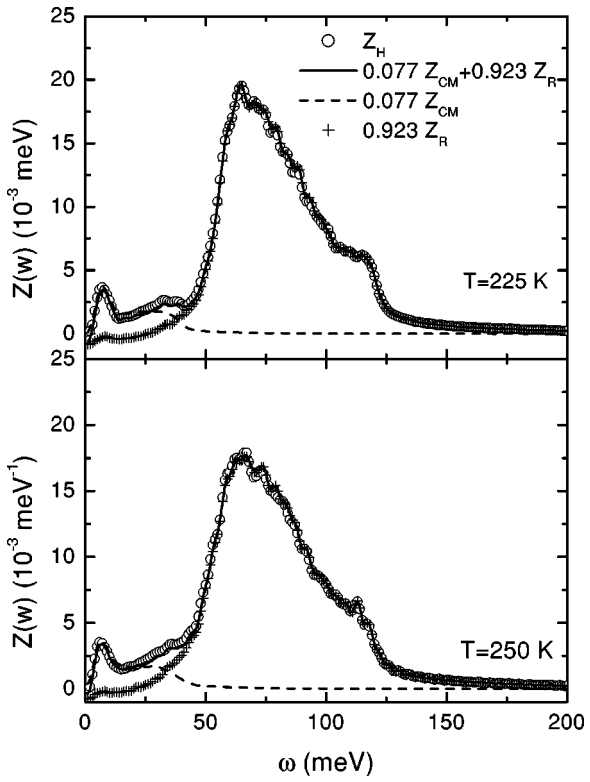

FIG. 3. Spectral density function of the normalized velocity autocorrelation function of the hydrogen atoms $Z_H(\omega)$, and its decomposition into the weighted sum of $Z_R(\omega)$ and $Z_{c.m.}(\omega)$, where the latter quantity represents the spectral density function of the normalized center-of-mass velocity autocorrelation function. It is to be noted that the prominent peak at 65 meV, the so-called hindered rotation peak, hardly shifts as a function of the temperature.

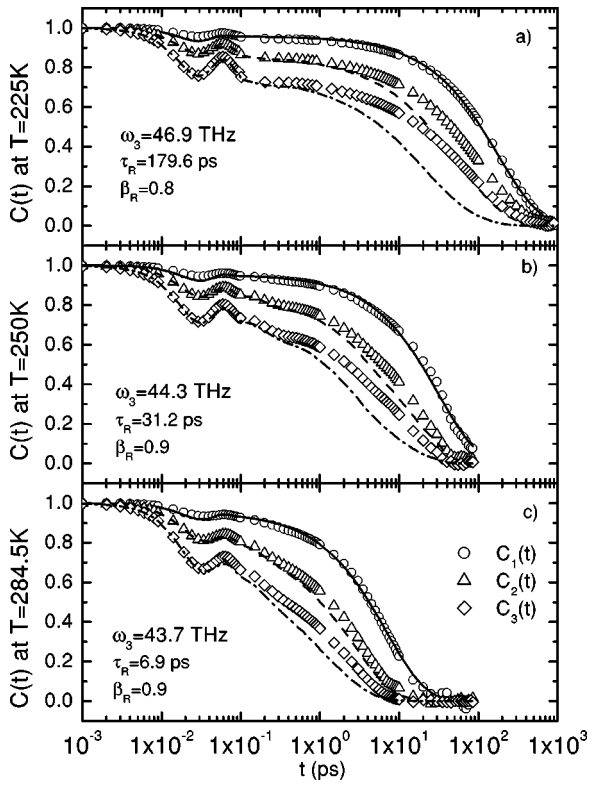

FIG. 4. The first three lowest-order rotational correlation functions, $C_1(t)$, $C_2(t)$, and $C_3(t)$, as a function of the time for three temperatures (225 K, 250 K, 284.5 K). The open circles represent simulated $C_1(t)$; the solid line, the fitted $C_1(t)$ by Eq. (18); the triangles, simulated $C_2(t)$; the dash line, the computed $C_2(t)$ by Eq. (22); the diamonds, simulated $C_3(t)$; the dash-dot line, the computed $C_3(t)$ by Eq. (23).

[17]. Densities in our simulation have been chosen on the basis of trial and error in preliminary runs. The corresponding pressures for the chosen final densities are reported in Table I, and it has been well described in [11].

III. DATA ANALYSIS

We start by discussing the validity of the decoupling approximation stated in Eq. (1). When dealing with a correlation function that is a product of four terms, each one with a (Q,t) dependence, it is always possible to rewrite it as the sum of all the possible binary factorizations of its terms plus another irreducible term, which we shall call the connected intermediate scattering function $F_{con}(Q,t)$. $F_{con}(Q,t)$ contains the contribution coming from the four factors coupled together in the correlation function and generally speaking it is different from zero. This procedure is applicable also to our correlation function. In fact, $F_H(Q,t)$ is the product of four factors

$$F_H(Q,t)=\langle e^{-i\vec{Q}\cdot\vec{R}(0)}e^{-i\vec{Q}\cdot\vec{b}(0)}e^{i\vec{Q}\cdot\vec{R}(t)}e^{i\vec{Q}\cdot\vec{b}(t)}\rangle. \quad (24)$$

Equation (24) can be written as

$$F_H(Q,t)-F_{con}(Q,t)=\langle e^{-i\vec{Q}\cdot\vec{R}(0)}e^{i\vec{Q}\cdot\vec{R}(t)}\rangle \times\langle e^{-i\vec{Q}\cdot\vec{b}(0)}e^{i\vec{Q}\cdot\vec{b}(t)}\rangle + \langle e^{-i\vec{Q}\cdot\vec{R}(0)}e^{i\vec{Q}\cdot\vec{b}(t)}\rangle \times\langle e^{i\vec{Q}\cdot\vec{R}(t)}e^{-i\vec{Q}\cdot\vec{b}(0)}\rangle. \quad (25)$$

The contributions, arising from all the terms composed of products of $\vec{R}$ and $\vec{b}$ variables at arbitrary times, are zero on average, due to the statistical independence between the two [18]. Therefore, the following relation holds [6]:

$$F_H(Q,t)=F_T(Q,t)F_R(Q,t)+F_{con}(Q,t), \quad (26)$$

where $F_{con}(Q,t)$ describes the strength of the coupling between translational and rotational motions as a function of Q and t, as observed by QENS.

In the graphs of Fig. 1 we show in a semilogarithmic scale the following five quantities: $F_{c.m.}(Q,t)$ [also denote as $F_T(Q,t)$], $F_H(Q,t)$, $F_{c.m.}(Q,t)F_R(Q,t)$, $F_{con}(Q,t)$ and $F_{c.m.}(Q,t)-F_H(Q,t)$. These functions are shown for a temperature 225 K at three Q values. These Q values are also quite close to the maximum and the minimum Q value that can be probed by a typical QENS experiment. We see that $F_H(Q,t)$ has the same short-time features as

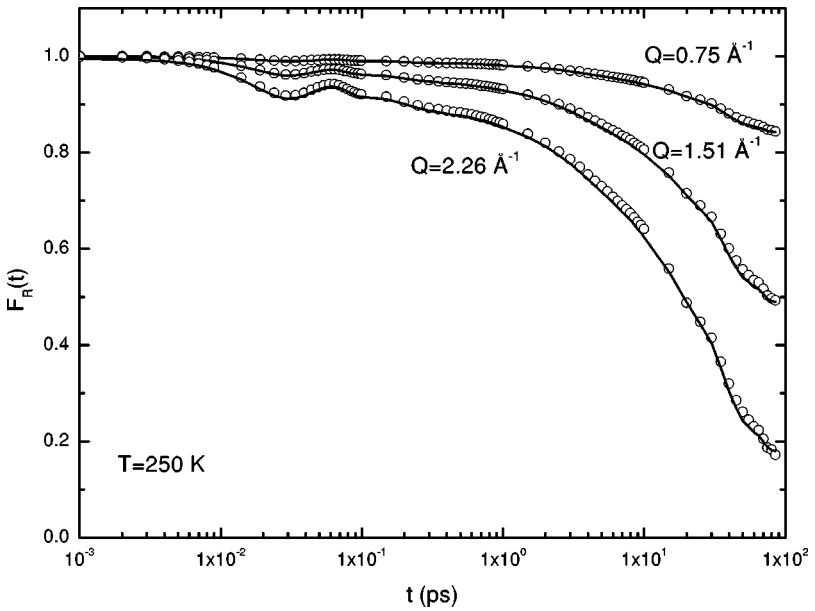

FIG. 5. Rotational intermediate scattering function $F_R(Q,t)$ vs time at three Q values and at $T=250$ K. From top to bottom, $Q=7.54$ nm^{-1}, 15.1 nm^{-1}, and 22.6 nm^{-1}. The open circles represent simulated $F_R(Q,t)$ at each Q value; the solid lines, the results computed by the Sears expansion Eq. (7) up to fourth-order term using simulated $C_1(t)$, $C_2(t)$, and $C_3(t)$.

$F_{c.m.}(Q,t)F_R(Q,t)$ but the same long-time feature as $F_{c.m.}(Q,t)$. So that $F_{con}(Q,t)$ is very small at times smaller than 1 ps but becomes non-negligible for long times. On the contrary $F_{c.m.}(Q,t)-F_H(Q,t)$ is negligible at times longer than 1 ps but large at short times. Both $F_{con}(Q,t)$ and $F_{c.m.}(Q,t)-F_H(Q,t)$ increase substantially with the increasing of Q value, but never reach 0.09 in magnitude.

We next discuss the validity of $C_1(t)$ as given by Eqs. (15) and (18). Since the short-time behavior $C_1^s(t)$ is essentially determined by the spectral density function of the normalized angular velocity autocorrelation function $Z_R(\omega)$ [Eq. (15)], we show in Fig. 2 the MD data of $Z_R(\omega)$ and its representation by an analytical function.

As shown in the preceding section, the simulated $Z_R(\omega)$ can be fitted by the Gaussian form $[2\omega^6/(15\omega_3^6\sqrt{2\pi\omega_3^2})]\exp[-\omega^2/(2\omega_3^2)]$. It is obvious that a broadband is peaked at ~ 65 meV for the MD data. In the Gaussian representation by Eq. (16), the peak position is at $\sqrt{6}\omega_3$. We note that this analytical function is a fair representation of the spectral density function.

We can show in the following that $Z_R(\omega)$ is part of the spectral density function of the hydrogen atom. Since we know

$$\vec{v}_H(t)=\vec{v}_{c.m.}(t)+\vec{v}_R(t) \tag{27}$$

and

$$\vec{v}_R(t)=b\vec{\omega}(t), \tag{28}$$

we get the relation

$$\langle\vec{v}_H(0)\cdot\vec{v}_H(t)\rangle=\langle\vec{v}_{c.m.}(0)\cdot\vec{v}_{c.m.}(t)\rangle+b^2\langle\vec{\omega}(0)\cdot\vec{\omega}(t)\rangle \tag{29}$$

in which we neglect the cross terms because they are very small compared to others at short times. Thus one can write

$$Z_H(\omega)\simeq\alpha Z_{c.m.}(\omega)+\beta Z_R(\omega), \tag{30}$$

where

$$Z_H(\omega)=\frac{1}{\pi}\int_{-\infty}^{\infty}e^{i\omega t}\frac{\langle\vec{v}_H(0)\cdot\vec{v}_H(t)\rangle}{\langle {v_H}^2\rangle}dt, \tag{31}$$

$$Z_{c.m.}(\omega)=\frac{1}{\pi}\int_{-\infty}^{\infty}e^{i\omega t}\frac{\langle\vec{v}_{c.m.}(0)\cdot\vec{v}_{c.m.}(t)\rangle}{\langle {v_{c.m.}}^2\rangle}dt, \tag{32}$$

and

$$\alpha+\beta=1.$$

In Fig. 3 we plot MD data for $Z_H(\omega)$ and its decomposition into sum of $Z_{c.m.}(\omega)$ and $Z_R(\omega)$ for two temperatures, $T=225$ K and $T=250$ K. It is obvious from the inspection of the figure that the two low-frequency peaks of the hydrogen density of states are translational in character and the prominent high-frequency peak is rotational in character. In the literature, it is often called the hindered rotation peak, which is clearly associated with the oscillation of the hydrogen atom perpendicular to its hydrogen bond.

In Fig. 4 we show the MD data for the first three rotational correlation functions $C_1(t)$, $C_2(t)$, and $C_3(t)$, for the three simulated temperatures. In comparison, we also show the results of our models for $C_1(t)$, $C_2(t)$, and $C_3(t)$ calculated by Eqs. (18), (22), and (23). We see that while the model for $C_1(t)$ agrees well with the MD data, the model for $C_2(t)$ and $C_3(t)$ do not show equally good agreements with the MD data, especially at long times. But, since at moderate Q values, contributions of $C_2(t)$ and $C_3(t)$ to the rotational ISF are not substantial, the calculated $F_R(Q,t)$'s still do not deviate substantially from the MD data as we shall show in later figures. Our model for the rotational correlation function, therefore, is satisfactory for the practical purpose of fitting the QENS data.

With the information of the complete time dependence of $C_1(t)$, $C_2(t)$, and $C_3(t)$, we are now ready to compute the rotational ISF using Sears expansion [Eq. (7)]. Figure 5

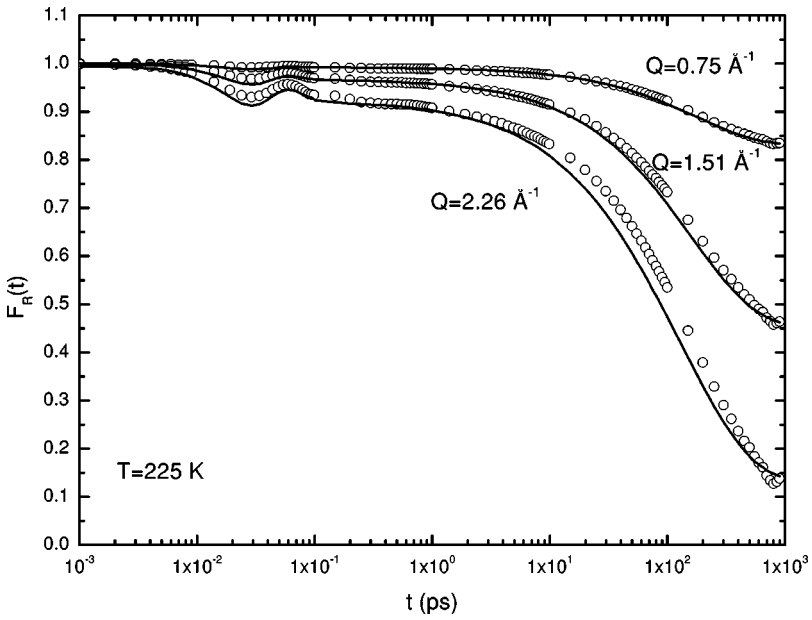

FIG. 6. Rotational intermediate scattering function $F_R(Q,t)$ vs time at three Q values (7.54 nm^{-1}, 15.1 nm^{-1}, and 22.6 nm^{-1}) and at $T=225$ K. From top to bottom, $Q=7.54$ nm^{-1}, 15.1 nm^{-1}, and 22.6 nm^{-1}. The open circles represent simulated $F_R(Q,t)$ at each Q value; the solid lines, the results computed by the Sears expansion using the theoretically generated $C_1(t)$ [Eq. (18)], $C_2(t)$ [Eq. (22)], and $C_3(t)$ [Eq. (23)].

shows the rotational ISF calculated by MD at three Q values and their computation by Sears expansion using the MD-generated $C_1(t)$, $C_2(t)$, and $C_3(t)$. One sees good agreements between the two, for all the three Q values, indicating that up to $Q=2.26$ Å^{-1}, the Sears expansion can be safely truncated at the fourth term.

Finally in Fig. 6 we show the comparison of the MD data for the rotational ISF at $T=225$ K with Sears expansion using our models for $C_1(t)$, $C_2(t)$, and $C_3(t)$. One sees that the agreements of the two are quite satisfactory for the practical purpose of QENS data analysis.

IV. CONCLUSION

In this paper we have shown that the decoupling approximation for the ISF $F_H(Q,t)$ is an acceptable approximation for analyses of QENS data from water in bulk or in a confined geometry. More precisely, the decoupling approximation is excellent up to $t=0.5$ ps and progressively becomes poorer for times longer than 1 ps. However, the maximum deviation does not exceed 0.09 even for large Q. If we accept this approximation, then we only need to compute $F_{c.m.}(Q,t)$ and $F_R(Q,t)$ separately. We already have a good analytical model for the former quantity, called the relaxing cage model [8]. In the relaxing cage model, an essential input quantity to the theory is the translational density of states of the hydrogen atom, which consists of two peaks, one at 7 meV and the other at 40 meV (see Fig. 3). We propose in this paper an analytical theory for the rotational ISF, in terms of the three lowest-order rotational correlation functions. We show that, in general, our theory for $C_1(t)$, $C_2(t)$, and $C_3(t)$ shows good representations of the corresponding MD-generated correlation functions. When they are used in conjunction with the Sears expansion to compute $F_R(Q,t)$, it shows good agreements with MD-generated ISF's. One essential ingredient in the theory for $C_1(t)$ is the spectral density function of the angular velocity autocorrelation function. We show that this spectral density function is nothing but the hindered rotation peak in the density of states of the hydrogen atom. The long-time behavior of $C_1(t)$ is modeled by a stretch exponential decay, which represents the relaxation of the hydrogen-bonded nearest-neighbor cage. Thus our models, both translational and rotational ISF's, make use of the basic property of water through the hydrogen atom density of states. Since the decoupling approximation is excellent at short times, our theory can, in principle, compute the dynamic structure factor up to an energy transfer of 120 meV or so, well into the inelastic scattering region of the spectrum. We shall, in the future, publish results of the analysis of QENS spectra as well as inelastic spectra from water using this theory.

ACKNOWLEDGMENTS

We are grateful to Francsco Sciortino for providing us with an SPC/E water simulation package and for instructions on how to use the package. We thank Ciya Liao for generous advice during the course of the simulation work.

[1] S.-H. Chen, in *Hydrogen-Bonded Liquids*, Vol. 329 of *NATO Advanced Studies Institute Series*, edited by John C. Dore and Jose Teixeira (Kluwer Academic, Dordrecht, 1991), pp. 289–332.

[2] S.-H. Chen, P. Gallo, and M.-C. Bellissent Funel, Can. J. Phys. **73**, 703 (1995).

[3] M.-C. Bellissent-Funel, S.-H. Chen, and J.-M. Zanotti, Phys. Rev. E **51**, 4558 (1995).

[4] S. Takahara, M. Nakano, S. Kittaka, Y. Kuroda, T. Mori, H. Hamano, and T. Yamaguchi, J. Phys. Chem. **103**, 5814 (1999).

[5] P. A. Egelstaff, *Thermal Neutron Scattering* (Academic Press, New York, 1971).
[6] S.-H. Chen, P. Gallo, F. Sciortino, and P. Tartaglia, Phys. Rev. E **56**, 4231 (1997).
[7] J. Teixeira, M.-C. Bellissent-Funel, S.-H. Chen, and A. J. Dianoux, Phys. Rev. A **31**, 1913 (1985).
[8] S.-H. Chen, C. Liao, F. Sciortino, P. Gallo, and P. Tartaglia, Phys. Rev. E **59**, 6708 (1999).
[9] J.-M. Zanotti, M.-C. Bellissent-Funel, and S.-H. Chen, Phys. Rev. E **59**, 3084 (1999).
[10] P. Gallo, F. Sciortino, P. Tartaglia, and S.-H. Chen, Phys. Rev. Lett. **76**, 2730 (1996).
[11] F. Sciortino, P. Gallo, S.-H. Chen, and P. Targaglia, Phys. Rev. E **54**, 6331 (1996).
[12] V. F. Sears, Can. J. Phys. **45**, 237 (1967).
[13] B. J. Berne, P. Pechukas, and G. D. Harp, J. Chem. Phys. **49**, 3125 (1968).
[14] G. L. Squires, *Introduction to the Theory of Thermal Neutron Scattering* (Cambridge University Press, Cambridge, 1978).
[15] Allen S. Weinrub, Ph.D. thesis, Harvard University, 1971.
[16] O. Steinhauser, Mol. Phys. **45**, 335 (1982).
[17] H. J. C. Berendsen *et al.*, J. Chem. Phys. **81**, 3684 (1984).
[18] The time dependence of $\vec{b}(t)$ is independent of the choice of the reference system. In the reference system defines by the molecular center of mass $\vec{R}(t)$, all mixed correlation functions vanish.